Simulation Study on the Effects of Operating Temperature on Cell Electrodes in Solid Oxide Fuel Cells

Xuan Vien Nguyen[1]*, An Quoc Hoang[2], Hong Son Nguyen Le[2]
[1]Department of Renewable Energy,
HCMC University of Technology and Education, Ho Chi Minh City, Viet Nam
[2]Department of Thermal Engineering,
HCMC University of Technology and Education, Ho Chi Minh City, Viet Nam
*Email: viennx@hcmute.edu.vn

Abstract

In this study, a three−dimensional numerical simulation on electrodes in solid oxide fuel cells (SOFCs) is investigated in both regular cell and button cell configurations. The cell unit models with a regular cell with an active area of 5cm $\times$ 5cm and with a button cell with an active area of 2.54 cm^2 were conducted to investigate the voltage distribution on cell electrodes in the solid oxide fuel cells (SOFCs). The performance characteristics in SOFC cell unit are determined through a numerical simulation method by using a computational fluid dynamic (CFD). The COMSOL Multiphysics software is used to investigate the model. The results show that the cell voltage in both regular cell and button cell with operating temperatures of 650 and 700 °C were lower than those at 750 °C. This means that when the operating temperature increases, the voltage and current density on the solid oxide fuel cell electrodes increases, and the performance of the cell is also improved.

Keywords: Solid oxide fuel cell, numerical simulation, electrodes, voltage distribution, cell performance.

1. Introduction

Nowadays, along with the advancement in science and technology, environmental and energy-saving issues have also become the paramount concern to improve people's quality of life. Increasing fossil fuel depletion and excessively high environmental pollution in the process of burning fuel and releasing carbon dioxide (CO_2) have been contributing to global warming, leading to negative changes in nature. Additionally, fossil fuels always have numerous potential harmful substances causing human diseases. Therefore, a wide range of solutions have been conducted to tackle the above issue, in which finding new sources of energy is considered an essential requirement. In particular, renewable energy sources and fuel cell energy sources are being strongly developed because of many advantages in terms of efficiency, convenience, and environmental friendliness [1-3].

The model supported anodes of solid oxide fuel cell (SOFC) is studied by using COMSOL Multiphysics software. The results indicated the position of maximum temperature distribution and maximum temperature slope, as well as the model performance parameters [4]. A numerical simulation model was developed to visualize and better understand various distributions such as gas concentration and temperature in solid oxide fuel cells (SOFCs) [5].

The modeling and simulations are implemented by using COMSOL Multiphysics. Simulations indicated some promising features and performance improvements of SOFC [6]. Temporal variation of the output voltage was investigated [7]. A three-dimensional model for a planar anode-supported SOFC was developed, which includes governing equations for momentum, heat, electron and ion transport. The results showed that the strength of stress of cell tends to be enlarged under fixed constraint conditions [8].

In the present study, the voltage distribution on cell electrodes in solid oxide fuel cells (SOFCs) through three-dimensional numerical simulation method is carried out using COMSOL Multiphysics. The algorithm of this software is based on the finite element method. The effects of different operating with the input temperatures of 650, 700, and 750 ºC on the cell performance are considered in this paper.
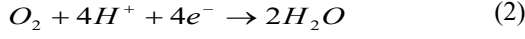
2. Methodology

2.1. Mathematic Equation

This model includes adjustment equations to simulate the exchange behaviors, charge and temperature of the species, as well as the constitutive correlation to calculate the flow density. The anode and cathode electrochemical reactions in the cell are shown in following equations [9,10].

For anode:

$$2H_2 \rightarrow 4H^+ + 4e^- \tag{1}$$

For cathode:

$$O_2 + 4H^+ + 4e^- \rightarrow 2H_2O \tag{2}$$

The energy equation can be described using the conduction equation to obtain the temperature distribution in the cell [11].

$$\nabla \cdot (-k^{eff} \nabla T) = \left[\frac{A}{V}\right]_{eff} S_T \tag{3}$$

Electrochemical reactions can be reasonably assumed to occur at the electrode/electrolyte interface. In the electrode, the Ohm's law is used to treat the transport of electronic charge and ionic charge, respectively.

$$-\nabla \cdot (\sigma_e^{eff} \nabla_{\varphi_e}) = \left[\frac{A}{V}\right]_{eff} S_e \tag{4}$$

$$-\nabla \cdot (\sigma_i^{eff} \nabla_{\varphi i}) = \left[\frac{A}{V}\right]_{eff} S_i \tag{5}$$

In (3), (4), (5), σ_e^{eff} and σ_i^{eff} are the effective electron conductivity and the ionic conductivity, respectively. k^{eff} is the effective thermal conductivity and includes the thermal conductivity of pores and solid materials, $\left[\frac{A}{V}\right]_{eff}$ is the specific surface area, which is the electrochemical reaction active area per unit volume, S_T is source term at pressure of 1atm and temperature of 273 K.

Butler-Volmer charge transfer kinetics describes the charge transfer current density. The charge transfer kinetics are shown in following equations [12]:

$$i_{a,ct} = i_{0,a} \left(\frac{c_{h2}}{c_{h2,ref}} \exp\left(0.5\frac{F}{RT}\eta\right) - \frac{c_{H_2O}}{c_{H_2O,ref}} \exp\left(\frac{-1.5F}{RT}\eta\right) \right) \tag{6}$$

$$i_{i,ct} = i_{0,c} \left(\exp\left(3.5\frac{F}{RT}\eta\right) - xo_2 \frac{c_t}{c_{O_2,ref}} \exp\left(\frac{-0.5F}{RT}\eta\right) \right) \tag{7}$$

where F is the Faraday's constant, R is the universal gas constant, η is the overpotentials, c_i and $c_{i,ref}$ represents the molar concentrations and reference concentrations and x_{O2} is the molar fraction of oxygen.

Species conservation equation is written as:

$$\nabla \cdot (\rho \omega_i \vec{u}) = \nabla \cdot (\rho \frac{\omega_i}{x_i} D_i^{eff} x_i) + \dot{R}_i \tag{8}$$

where $\dot{R}_i$ is mass production rate of species i, x_i is molar fraction of species i, ω_i is mass fraction of species i.

Mass conversion equation is written as:

$$\nabla \cdot (\rho \vec{u}) = \dot{W} \tag{9}$$

where $\dot{W}$ is mass source.

Momentum conservation equation:

$$\nabla \cdot (\frac{\rho \vec{u} \vec{u}}{\varepsilon}) = -\varepsilon \nabla p + \nabla \cdot [\mu(\nabla \vec{u} + \nabla \vec{u}^T) - \frac{2}{3}\mu\nabla\vec{u}] + \varepsilon \vec{F}_{Da} \tag{10}$$

where ε is porosity, μ is dynamic viscosity of species, $\vec{F}_{Da}$ is Darcy's friction force.

2.2. Model Establishment and Mesh Generation

The model used to simulate the voltage distribution on cell electrode is implemented with cell having an active area of 5 cm ×5 cm for regular cell (as shown in Fig. 1a) and a button cell with an active area of 2.54 cm^2 (as shown in Fig. 1b).
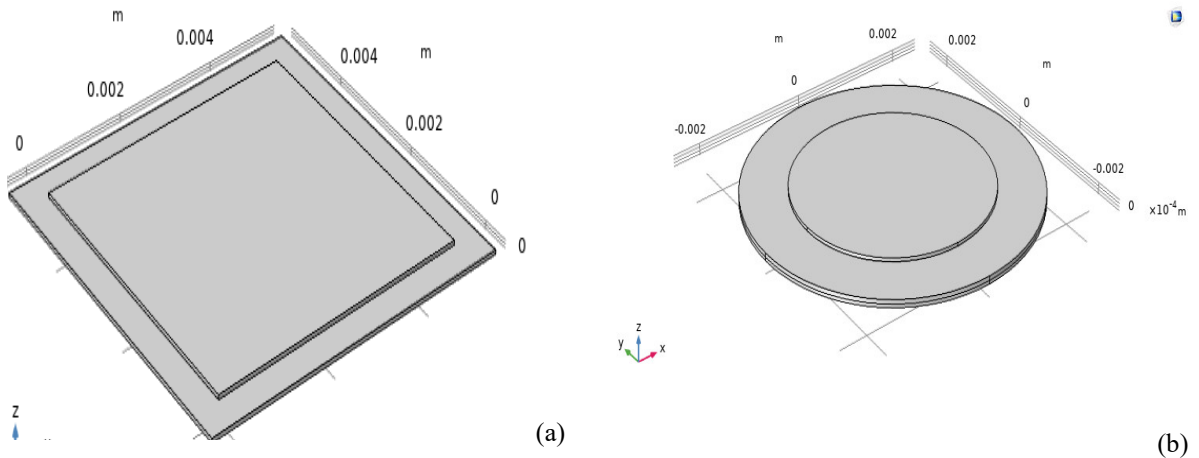

Fig. 1. The simulation model of a) regular cell b) button cell

The structure diagram of electrode layers in an cell unit is shown in Fig. 2. After setting boundary conditions and physical establishment for the model, the model is meshed according to appropriate input and output dimensions with the model shape in accordance with individual dimensions of each electrolyte layer and boundary layers of the model. In regular cell model, the O_2 flow rate of 400 ml/min on the cathode surface and H_2 flow rate of 200 ml/min (3% water) on the anode surface are supplied. In button cell model, the O_2 flow rate of 150 ml/min on the cathode surface and H_2 flow rate of 100 ml/min (3% water) on the anode surface are used.
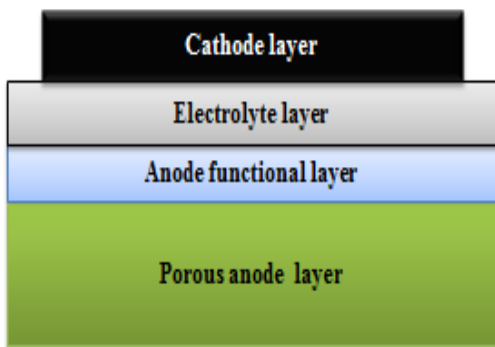

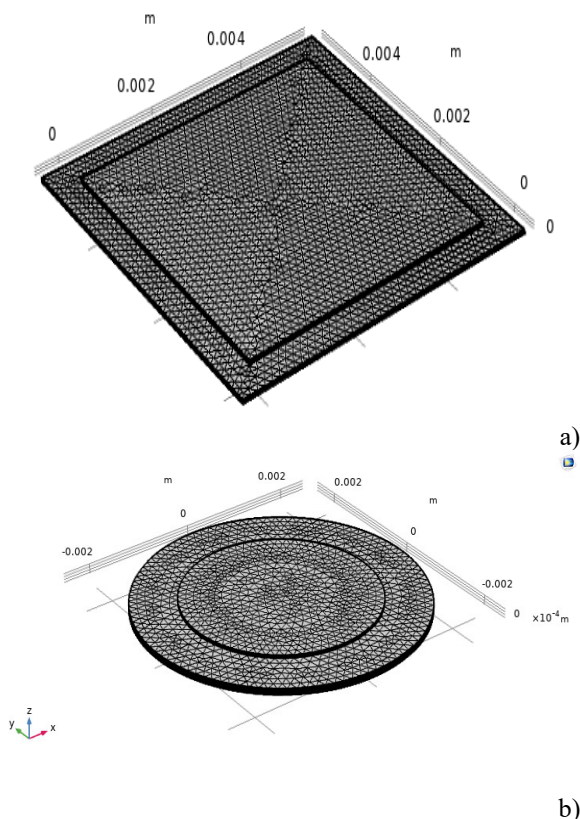Fig. 2. Structure of the SOFC cell unit

a)

b)

Fig. 3. Mesh generation of a) regular cell; b) button cell unit

Fig. 3 indicates the meshing of the SOFC cell unit model. Since the model shape is not too complicated with flat boundary edges, the meshing model selected the linear elements as triangles with straight sides on the model.

2.3. Boundary Conditions

The boundary conditions for the inlet gas channels are defined as pressure with no viscous stress. The gas mixture at the anode inlet is 97% H_2 and 3% H_2O. On the cathode side, O_2 is supplied into the system. Zero flux is specified at the end of the electrodes and electrolyte. The pressures are fixed as atmospheric pressure (1atm). The boundary conditions at the exits are limited as convective flux. The temperature boundary condition at the inlets of anode and cathode flow channels is set to the operating temperature of 650 °C, 700 °C and 750 °C. The voltage at the anode current collector is set to zero and to the working cell voltage at the cathode current collector.

3. Results and Discussion

3.1. The distribution of Voltage on the Regular Cell at the Different Temperatures

To investigate the influence of the temperature on the performance of the SOFC, simulations were conducted for this model with the O_2 flow rate of 400ml/min on the cathode surface and H_2 flow rate of 200ml/min on the anode surface. Figure 4 shows the voltage difference on the regular cells at 650 ºC, 700 ºC and 750 ºC. As shown in Fig. 4, the cell voltage with operating temperatures of 650 ºC and 700 °C were lower than those at 750 °C. This means that when the input temperature increases, the voltage on the SOFC surface increases and the performance of the fuel cell is improved.

Figure 5 shows the current density and voltage of SOFC operating at different temperatures. The simulation results show that the cell voltages were 0.95 V, 0.98 V, and 1.05 V at 650 ºC, 700 ºC, and 750 ºC, respectively. The maximum current densities of the cell were found to be 350.3 mW/cm², 456.05 mA/cm², and 579.08 mW/cm² with operating temperatures of 650 ºC, 700 ºC, and 750 ºC, respectively. From the comparison, it can be clearly seen that the simulation result is suitable for the theoretical values. When the operating temperature of the cell rises, the current density and voltage of the cell also increase, causing the performance of SOFC cells to improve. This happens due to the increase in the ionic conductivity in the electrolyte and electrochemical reaction to the electrode at higher temperatures.
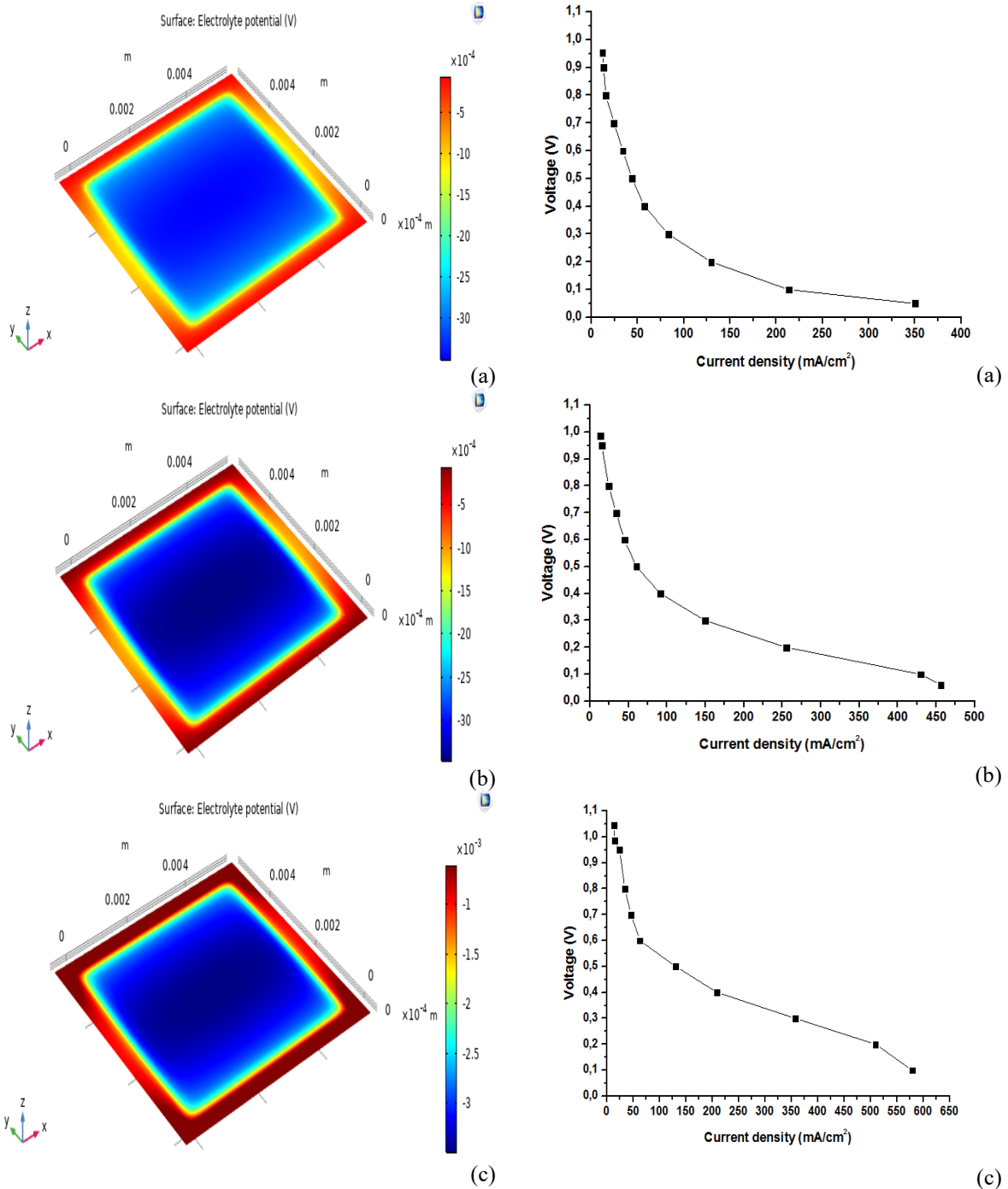
Fig. 4. The distribution of voltage on the SOFC cells at the temperatures of a) 650 ºC; b) 700 ºC; c) 750 ºC

Fig. 5. The voltage and current density on the SOFC regular cells at the temperatures of a) 650 ºC; b) 700 ºC; c) 750 ºC

3.2. The Distribution of Voltage on the Button Cell at the Different Temperatures

Figure 6 depicts the voltage distribution on button cell electrode at operating temperatures of 650, 700, and 750 ºC. The results are similar with regular cell (shown in Fig. 4). This means that the operating temperature of the cell rises, the current density and voltage of the cell also increase. In Fig. 4 and 6, the highest voltage distributes in active area.

Fig. 7 shows the current density and voltage of button cell operating at different temperatures. The simulation results show that the cell voltages were 0.92 V, 0.96 V and 1.02 V at 650, 700, and 750 ºC, respectively. The maximum current densities of the cell were found to be 830.7 mW/cm², 932.6 mA/cm², and 1189.1 mW/cm² with operating temperatures of 650, 700, and 750 ºC, respectively.
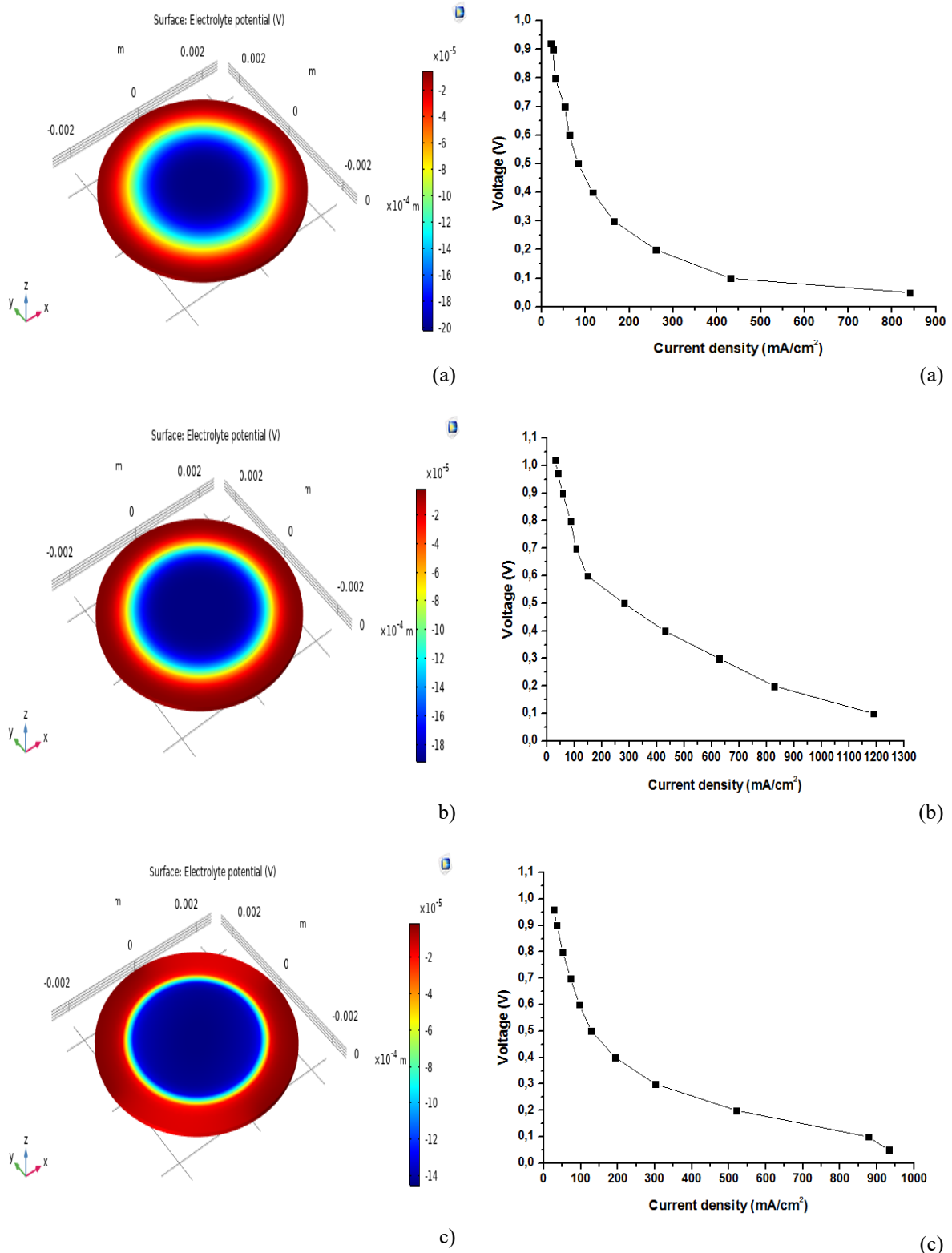
(a)

(a)

b)

(b)

c)

(c)

Fig. 6. The distribution of voltage on the SOFC button cells at the temperatures of a) 650 ºC; b) 700 ºC; c) 750 ºC

Fig. 7. The voltage and current density on the SOFC button cells at the temperatures of a) 650 ºC; b) 700 ºC; c) 750 ºC

3.3. The Experimental Performance of Regular Cell at the Different Temperatures

Regular cells were fabricated from anode–electrolyte tapes produced with sintering temperatures of 1400 °C. Graphs of the power generation of a 5cm × 5cm anode−supported single cell are shown in Fig. 8. The cell was operated using a hydrogen/3% water mixture as fuel and air as an oxidant. The performance of the anode−supported single cells was analyzed at an operating temperature of 650 ºC, 700 ºC and 750 °C. With an operating temperature of 650 ºC, open−circuit voltages (OCVs) of the single cell were observed to be around 1.0 V. The maximum observed power and current densities of the cell were found to be 104.6 mW/cm^2 and 395.84 mA/cm^2, respectively. The total output power was approximately 2.61 W, as shown in Fig. 8a. Figure 8b shows the cell performances with an operating temperature of 700 ºC. As shown in the figure, the maximum power and current densities of the cell were 135.6 mW/cm^2 and 461.25 mA/cm^2, respectively. The open−circuit voltages (OCVs) of the cell were around 1.0 V, and the total output power was approximately 3.39 W. As shown in Fig. 8c, the open−circuit voltages (OCVs) of the cell were around 1.01 V an operating temperature of 750 ºC. The maximum power density and current density of the cell were 178 mW/cm^2 and 620.8 mA/cm^2, respectively. The total output power was 4.45 W. The results show that the regular cell performances with operating temperatures of 650 and 700 °C were much lower than those with 750 °C. This result is mainly attributed to the fact that a operating temperature also affects the change in the activation of the cell. This is similar to the simulation in Fig. 5. Nevertheless, this investigation demonstrated the feasibility of using an operating temperature in SOFCs.

3.4. The Experimental Performance of Button Cell at the Different Temperatures

Cells were fabricated from anode–electrolyte tapes produced with a hot−pressing load of 3000 PSI and sintering temperatures of 1400 °C. A cell with an active reaction area of 2.54 cm^2 was used as the standard cell to test the power density. The OCV and power density of the single cell at operating temperatures of 650 ºC, 700 ºC and 750 °C are shown in Fig. 9. The OCVs of cell were around 1.05 V, and the maximum power densities of the cell were 245.7, 273.8, and 430.7 mW/cm^2 at operating temperatures of 650 ºC, 700 ºC and 750 °C, respectively. The maximum current densities of the cell were 785.4, 885.04, and 1252.4 mA/cm^2, resulting in total output powers of approximately 0.62, 0.71, and 1.09 W, respectively. The results show that the cell performances with operating temperatures of 650 and 700 °C were much lower than those at 750 °C. The cell performances are quite similar to simulation results. The optimal operating temperature of model is 750 °C.
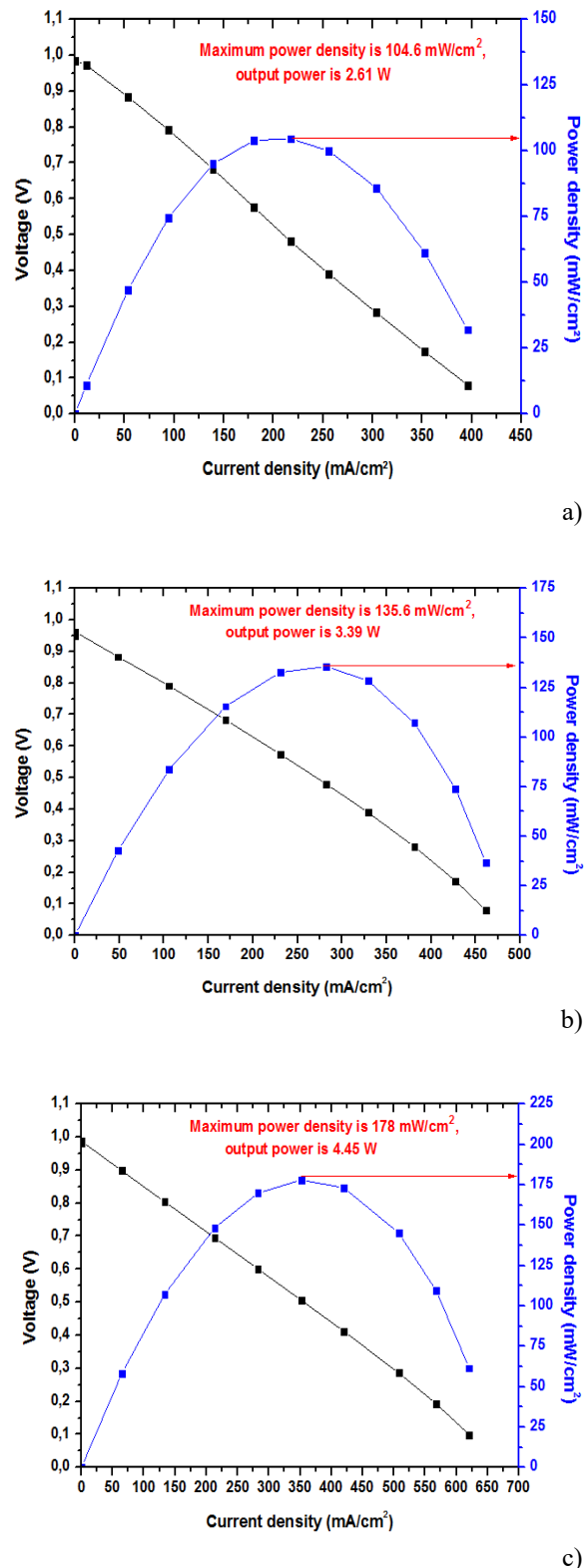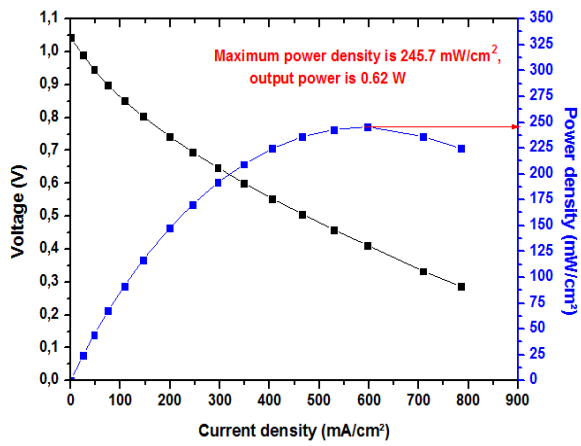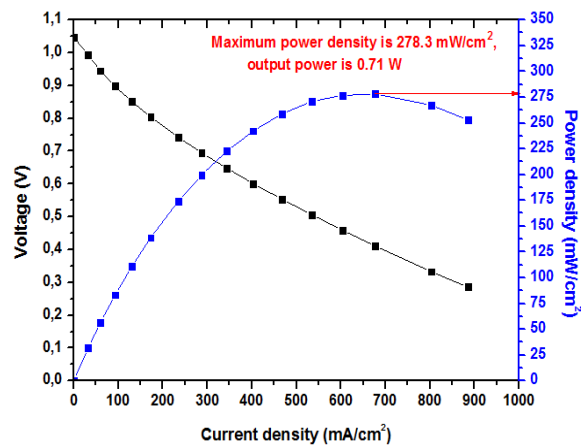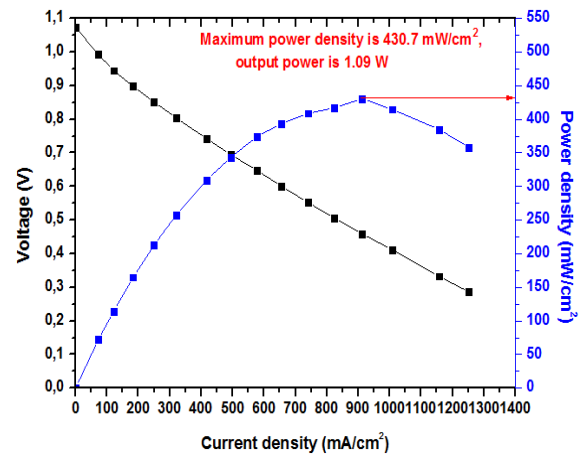

a)

b)

c)

Fig. 8. The IV–IP curves of regular cell with operating temperatures of a) 650 ºC; b) 700 ºC; c) 750 ºC

Fig. 9. The IV–IP curves of a button cell with operating temperature of a) 650 ºC; b) 700 ºC; c) 750 ºC

4. Conclusion

In this work, the voltage distribution on regular cell and button cell electrode in the solid oxide fuel cell (SOFC) is investigated by using numerical simulation method. The results show that the voltage distribution with operating temperatures of 650 and 700 °C was lower than those at 750 °C. The voltage of the regular cell were 0.95 V, 0.98 V and 1.05 V at 650, 700, and 750 ºC, respectively. The cell voltages of button cell were 0.92 V, 0.96 V and 1.02 V at 650, 700, and 750 ºC, respectively. The result shows when the operating temperature increases, the voltage on the SOFC surface increases and the performance of the fuel cell is improved. This means that there is an increase in the chemical reaction rate when the operating temperature rises.

Acknowledgments

References

[1] L. Blum, L.G.J. de Haart, J. Malzbender, *et al.*, Recent results in Jülich solid oxide fuel cell technology development, J. Power Sources, vol. 241 no. 1, Nov. 2013, pp. 477–485.
https://doi.org/10.1016/j.jpowsour.2013.04.110

[2] AnduJar JM, Segura F., Fuel cells: History and updating, A walk along two centuries, Renew and Sus Energy Reviews, vol. 13, no. 9, Dec. 2009, pp. 2309–2322.
https://doi.org/10.1016/j.rser.2009.03.015

[3] Mandeep Singh, DarioZappa, Elisabetta Comini., Solid oxide fuel cell: Decade of progress, future perspectives and challenges, Int. J. Hydrogen Energy, vol. 46, no. 54, Aug. 2021, pp. 27643−27674.
https://doi.org/10.1016/j.ijhydene.2021.06.020

[4] Marko Nerat, Đani Juricic, A comprehensive 3-D modeling of a single planar solid oxide fuel cell, Int. J. Hydrogen Energy, vol. 41, no. 5, Feb. 2016, pp. 3613−3627.
https://doi.org/10.1016/j.ijhydene.2015.11.136

[5] K.Takino, *et al.*, Simulation of SOFC performance using a modified exchange current density for pre-reformed methane-based fuels, Int. J. Hydrogen Energy, vol. 45, no. 11, Feb. 2020, pp. 6912−6925.
https://doi.org/10.1016/j.ijhydene.2019.12.089

[6] Jawad Hussain, Rashid Ali, Majid Niaz Akhtar, Modeling and simulation of planar SOFC to study the electrochemical properties, Current Applied Physics, vol. 20, no. 5, May 2020, pp. 660−672.
https://doi.org/10.1016/j.cap.2020.02.018

[7] Chaisantikulwat A, Diaz-Goano C, Meadows ES., Dynamic modelling and control of planar anode supported solid oxide fuel cell, Comp. Chem. Eng., vol. 32, no. 10, Oct. 2008, pp. 2365−2381.
https://doi.org/10.1016/j.compchemeng.2007.12.003

[8] MinXu, *et al.*, Modeling of an anode supported solid oxide fuel cell focusing on thermal stresses, Int. J. Hydrogen Energy, vol. 41, no. 33, Sep. 2016, pp. 14927−14940.
https://doi.org/10.1016/j.ijhydene.2016.06.171

[9] Young Jin Kim, Min Chul Lee, The influence of flow direction variation on the performance of a single cell for an anode-substrate flat-panel solid oxide fuel cell, Int. J. Hydrogen Energy, vol. 45, no. 39, Aug. 2020, pp. 20369−20381.
https://doi.org/10.1016/j.ijhydene.2019.10.129

[10] Congying Jiang, Yuchen Gu, Wanbing Guan, 3D thermo-electro-chemo-mechanical coupled modeling of solid oxide fuel cell with double-sided cathodes, Int. J. Hydrogen Energy, vol. 45, no. 1, Jan. 2020, pp. 904−915.
https://doi.org/10.1016/j.ijhydene.2019.10.139

[11] A. Su, Y.M. Ferng, C.B. Wang, C.H. Cheng, Analytically investigating the characteristics of a hightemperature unitized regenerative solid oxide fuel cell, Int. J. Energy Research, vol. 37, no. 13, Oct. 2013, pp. 1699–1708.
https://doi.org/10.1002/er.3071

[12] A.N. Celik. Three-dimensional multiphysics model of a planar solid oxide fuel cell using computational fluid dynamics approach. Int. J. Hydrogen Energy vol. 43, no. 42, Oct. 2018, pp. 19730−19748.
https://doi.org/10.1016/j.ijhydene.2018.08.212